ELSEVIER

Palaeogeography, Palaeoclimatology, Palaeoecology 189 (2003) 97–115

PALAEO

www.elsevier.com/locate/palaeo

Upper Cretaceous stable carbon isotope stratigraphy of terrestrial organic matter from Sakhalin, Russian Far East: a proxy for the isotopic composition of paleoatmospheric CO_2

Takashi Hasegawa [a,*], Lisa M. Pratt [b], Haruyoshi Maeda [c], Yasunari Shigeta [d], Takashi Okamoto [e], Tomoki Kase [d], Kazuhiko Uemura [d]

[a] *Department of Earth Sciences, Faculty of Science, Kanazawa University, Kakuma-machi, Kanazawa 920-1192, Japan*
[b] *Department of Geological Sciences, Indiana University, 1005 East10th St., Bloomington, IN 47406-1403, USA*
[c] *Department of Geology and Mineralogy, Graduate School of Science, Kyoto University, Sakyo-ku, Kyoto 606-8502, Japan*
[d] *Department of Geology and Palaeontology, National Science Museum, 3-23-1 Hyakunin-cho, Shinjuku-ku, Tokyo 169-0073, Japan*
[e] *Department of Biology and Earth Sciences, Faculty of Science, Ehime University, 2-5 Bunkyo-cho, Matsuyama 790-8577, Japan*

Received 27 November 2001; received in revised form 23 September 2002; accepted 25 October 2002

Abstract

Time-stratigraphic patterns of stable carbon isotopic ratios recorded in terrestrial organic matter from Cenomanian–Maastrichtian successions for the Russian Far East can be correlated to those of carbonate carbon from well-studied successions for other parts of the world. Age-indicative biostratigraphy based on regional ammonoids and inoceramid bivalves are well established in Japan and can be applied to the whole Cretaceous succession except for the Upper Cenomanian–Lower Turonian and the upper part of the Maastrichtian (zones lacking macrofossils). Globally correlative carbon isotopic events previously documented with carbonate carbon from Europe and with carbonate carbon and marine organic matter from the U.S. Western Interior are recognized with similar magnitude through uppermost Cenomanian–Lower Campanian. In ascending order these events are: positive 'spike' across the Cenomanian–Turonian boundary; step-like leveled segment followed by negative shift (Lower–Middle Turonian); trough-like negative excursion (Middle–Upper Turonian); positive rebound coupled with following broad peak (Coniacian); and positive peak (basal Campanian) followed by modest negative excursion. The parallel fluctuation of the $\delta^{13}C$ value between the terrestrial organic matter and carbonate suggests carbon isotopic equilibrium between surface seawater and atmospheric CO_2 and demonstrates that the isotopic curve of terrestrial organic carbon can be used to monitor carbon isotopic fluctuations of CO_2 in the ocean–atmosphere system. In the Upper Campanian and Maastrichtian, a negative $\delta^{13}C$ excursion within chron 33r and a following rapid rebound can be correlated with the same distinctive carbon isotopic feature of carbonate observed in the deep sea cores from South and North Atlantic, the Indian, and the Pacific Oceans. Within this interval, the $\delta^{13}C$ value of terrestrial organic matter also reflects carbon isotopic fluctuation of the global CO_2 reservoir with relatively minor regional/local 'noise'.

Keywords: carbon isotope; CO_2; Cretaceous; organic carbon; paleoenvironment; Sakhalin; terrestrial

* Corresponding author. Fax: +81-76-264-5746. *E-mail address:* jh7ujr@kenroku.kanazawa-u.ac.jp (T. Hasegawa).

0031-0182/02/$ – see front matter © 2002 Elsevier Science B.V. All rights reserved.
PII: S0031-0182(02)00634-X

1. Introduction

Time-stratigraphic fluctuations of stable carbon isotope ratios ($\delta^{13}C$) in carbonate are sometimes used as a proxy for carbon isotopic fluctuation of averaged seawater to understand the long-term state of the global carbon cycle and related paleoclimate. Many stratigraphic studies of carbonate carbon isotopes have been carried out on different Upper Cretaceous successions in this decade (e.g. Barrera and Huber, 1990; Corfield et al., 1991; Pratt et al., 1993; Jenkyns et al., 1994; Barrera and Savin, 1999; Stoll and Schrag, 2000); however, isotopic signals of carbonate carbon potentially record local oceanographic phenomena and/or are overwritten by secondary factors during diagenesis. To refine discussions about the global carbon cycle during the Late Cretaceous, time-series of carbon isotopic signals for the ocean-atmospheric reservoir should be reconstructed from data which are independent of carbonate carbon and should be verified. Arthur et al. (1988) discussed $\delta^{13}C$ fluctuation for marine organic matter (MOM) across the Cretaceous Cenomanian–Turonian (C–T) boundary. They interpreted the enhanced excursion of the $\delta^{13}C$ value observed in MOM relative to carbonate carbon as related to a decrease in pCO_2. Recent studies demonstrated that pCO_2 in ambient water and growth rate were the main factors controlling the $\delta^{13}C$ value of marine phytoplankton (Laws et al., 1995; Popp et al., 1998). MOM from sedimentary rocks cannot act as a monitor for a time-series of the $\delta^{13}C$ value of CO_2 in the ocean–atmosphere system because of the environment-dependent feature of the $\delta^{13}C$ value. On the other hand, carbon isotope stratigraphy of terrestrial organic matter (TOM) can play such a role. Carbon fixed by land plants should reflect carbon isotopic fluctuations of atmospheric CO_2 and, consequently, the isotopic behavior of the carbon reservoir of the ocean–atmosphere system. The objective of this study is to offer an Upper Cretaceous carbon isotope stratigraphy from TOM and to compare it with that from carbonate in order to verify that carbon isotopic fluctuations have affected the entire global ocean–atmosphere system.

Recently, Hasegawa (1997) and Gröcke et al. (1999) established a $\delta^{13}C$ stratigraphy from TOM through the Cenomanian–Turonian and Barremian–Albian respectively. Both studies employed marine successions with good age control and the authors recognized globally correlative isotopic features in their profiles. Hasegawa (1997) checked the composition of organic matter by petrographic study and demonstrated a strong predominance of higher terrestrial plant materials in his bulk-analyzed mudstone samples. Gröcke et al. (1999) used selected wood fragments from the strata for the analysis. From these studies of TOM, it is obvious that appropriate age control of a succession and recognition of terrestrial origin of samples are important prerequisites for a $\delta^{13}C$ stratigraphy of TOM in order to understand the ocean–atmosphere system of Earth's carbon cycle. For discussions on short-term disturbance of the steady state of the system, age control with a resolution less than 100 kyr is required (e.g. Kump and Arthur, 1999; Kuypers et al., 1999). With long-term fluctuations of the steady state, on the other hand, interregional correlations with a stage-level resolution within the biostratigraphic uncertainty is still practical for the Upper Cretaceous because the wavelength of the $\delta^{13}C$ fluctuation is similar to or longer than durations of the stages (Jenkyns et al., 1994). The Late Cretaceous is the best-known period of warm and equable climate during the Phanerozoic (e.g. Frakes et al., 1992) and offers important information for understanding general features of the long-term global carbon cycles. In spite of such importance, Cretaceous carbon isotope stratigraphy of TOM stratigraphically above the Turonian has never been studied before.

This study addresses the following subjects: (1) correlation of local lithostratigraphy to establish a composite section; (2) petrographic examination of kerogens in mudstone to demonstrate a terrestrial origin; (3) documentation of $\delta^{13}C$ stratigraphy of TOM from the Middle Cenomanian through Maastrichtian; (4) comparison of $\delta^{13}C$ profiles between TOM and carbonate from Europe (Jenkyns et al., 1994), the U.S. Western Interior (Hayes et al., 1989; Pratt et al., 1993) and the South Atlantic (ODP 690C; Barrera and Huber, 1990); (5) discussion of non-global carbon

isotope signals from TOM possibly controlled by land plant-specific factors for carbon isotope fractionation; and (6) discussion of the amplitude of isotopic events in order to discriminate between local or regional isotopic signals and global features. The amplitude is indispensable for evaluation of possible pCO_2 effects on carbon isotopic fractionation during production of TOM.

The Naiba area (Fig. 1) was chosen for this study because of its nearly continuous exposure, stable depositional environment through the Middle Cenomanian–Lower Campanian sequence, and the predominance of terrestrial kerogen in mudstone.

2. Geologic setting

Upper Cretaceous strata in the Naiba area were comprehensively studied by Matsumoto (1942) and divided into two groups. Vereshchagin (1961) recognized that Matsumoto's group boundary was not an unconformity but a conformity and defined two formations, named the Bykov Formation and Krasnoyarka Formation in an ascending order. Salnikov and Tikhomolov (1987) and Kodama et al. (2002) summarized the geology of this area in detail. A geological map of the studied area is shown in Fig. 1.

The Bykov Formation consists of a dark gray mudstone facies with occasional intercalations of bentonite and turbiditic sandstone layers and is correlated to the upper part of the Yezo Group distributed in Hokkaido, Japan. Well-preserved ammonoid and inoceramid bivalve fossils occur within the formation except for the lower part. The lowermost part of the formation is composed of siltstone or sandy siltstone. Intercalations of tuffaceous sandstone layers, less than 3 m thick, were observed within a stratigraphic interval of less than 40 m near the base of the Bykov Formation ('Shadrinka Sandstone') offering an excellent key horizon for local correlation that separates overlying facies from the siltstone. A correlative tuffaceous lithology is widely observable in Lower Turonian strata in Hokkaido, Japan (e.g. Tanabe et al., 1977; Maeda, 1987; Motoyama et al., 1991; Kaiho and Hasegawa, 1994; Hasegawa, 1995; Wani and Hirano, 2000). Above the tuffaceous sandstone layers, there is a finer-grained, laminated, clayey siltstone of a more distal nature. Fine lamination and occasionally preserved *Chondrites* and/or *Planolites*-like ichnofossils but an absence of macrofossils in this siltstone (*Planolites* mudstone; Maeda, 1987) indicate limited activity of benthic organisms. This *Planolites* mudstone facies is horizontally widespread but stratigraphically limited to the Lower Turonian in Japan (Maeda, 1987; Hasegawa, 1997; Shibata et al., 1997). The clayey siltstone with *Planolites* mudstone facies gradually becomes less clayey through the middle of the formation and becomes rather sandy near the top, suggesting gradual change from distal to proximal depositional environments. In the upper sandy part, exotic limestone blocks, containing shallow marine gastropods and trigoniid bivalves, are recognized in the mudstone. These characteristics of the Bykov Formation conspicuously resemble the correlative interval of the Yezo Group (Motoyama et al., 1991), which is interpreted as a fore-arc basin sediment (Okada, 1979, 1983). The Bykov Formation is also interpreted as a fore-arc basin sediment from a depositional setting similar to the Yezo Group. It conformably overlies the underlying Naiba Formation, which is composed mainly of stratified sandstone with some intercalations of sandy siltstone.

The Krasnoyarka Formation conformably overlies the Bykov Formation and is composed of volcanogenic sandstones alternating with sandy siltstones that are interpreted to be deposited in a deltaic environment. Minor intervals of non-deposition or condensation may exist in this formation but their duration is shorter than biostratigraphic or magnetostratigraphic resolution. Tertiary strata unconformably overlie the Krasnoyarka Formation.

3. Chronology

Although international stage-diagnostic species are few, ammonoids and inoceramid bivalves of the North Pacific realm occur abundantly in Cretaceous deposits in the Naiba area (e.g. Matsumo-

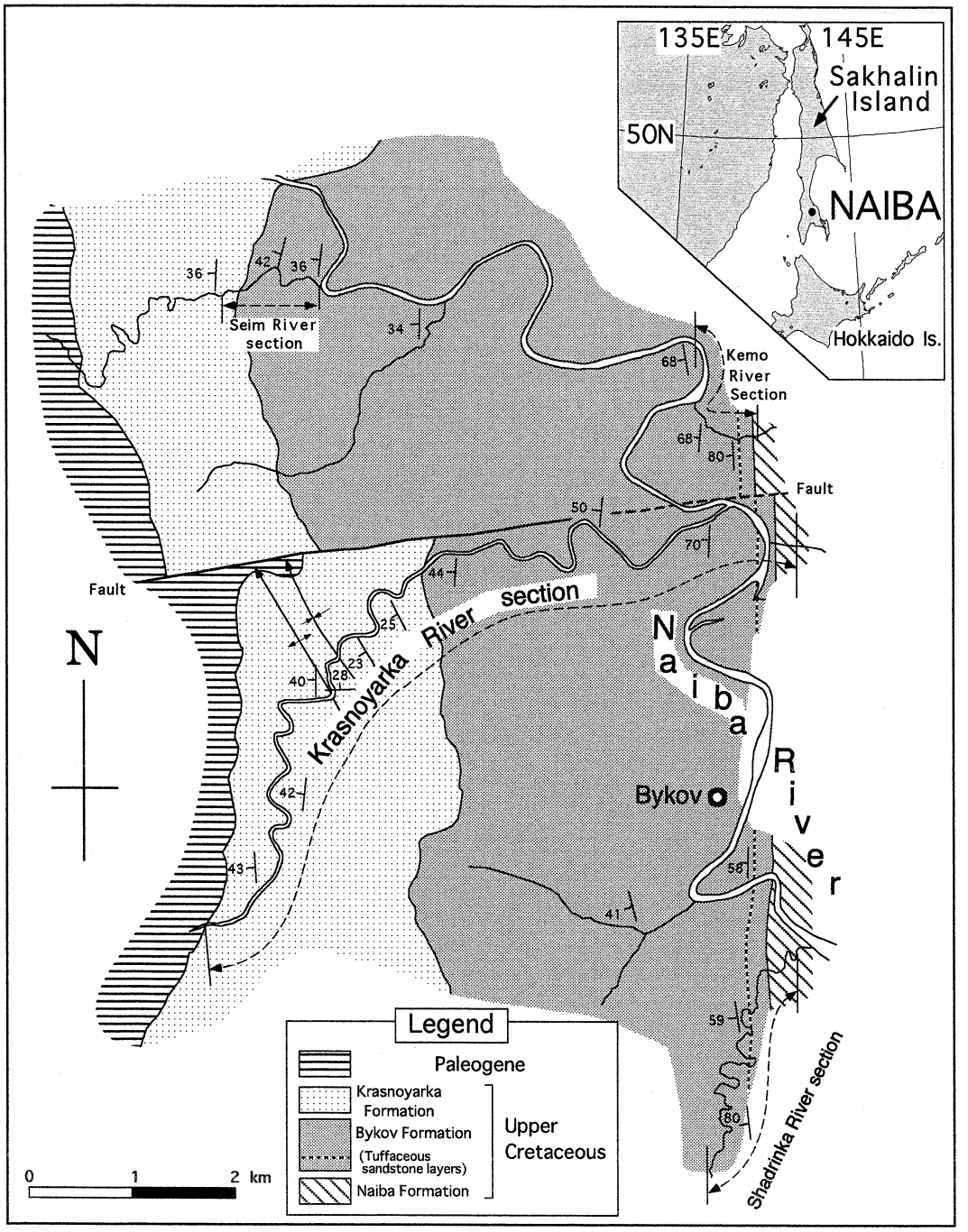

Fig. 1. Geological map showing distribution of the Upper Cretaceous rocks in the Naiba area, Sakhalin Island, Russia. Studied sections are indicated with broken lines and arrows. The locality of the studied area is also shown (upper right).

to, 1942; Mirolybov, 1987; Zonova, 1987; Kodama et al., 2002). The Naiba molluscan assemblages are closely similar to those of the Yezo Group in Hokkaido, Japan (e.g. Matsumoto, 1942, 1954, 1959; Matsumoto et al., 1985, 1991; Toshimitsu et al., 1995), allowing good biostratigraphic correlation between these areas (Shigeta et al., 1999; Kodama et al., 2002). On this basis, the four studied sections logged in this paper can be correlated to the Middle Cenomanian through Maastrichtian (Fig. 2).

Desmoceras (*Pseudouhligella*) *japonicum* and *Inoceramus* aff. *pennatulus* occur abundantly in the uppermost part of the Naiba Formation (alternating beds of siltstone and sandstone) exposed along the lowermost course of the Shadrinka River (Fig. 1). Just above this level in the lowest Bykov Formation, *Calycoceras* sp. and *Puzosia nipponica* occur together with *I.* aff. *pennatulus*. These assemblages strongly suggest a Middle Cenomanian age (Toshimitsu et al., 1995).

Macrofossils were not recovered from the overlying clayey siltstone in the lower part of the Bykov Formation (zone lacking macrofossils in Fig. 2). However, the clayey siltstone did yield numerous *Chondrites* and/or *Planolites*-like burrows as well as intercalations of bluish dark gray laminae.

Inoceramus hobetsensis and *Romaniceras yubarense* are indicatives of the Middle Turonian in the Far Eastern realm and occur in the lower middle part of the Bykov Formation along the upper course of the Shadrinka River, the lower course of the Krasnoyarka River, and the Kemo River (Figs. 1, 2). They are succeeded by *Nipponites mirabilis* and *Scalarites scalaris* suggesting a Middle to Late Turonian age (Matsumoto, 1977), supported by occurrences of the Late Turonian *Inoceramus tenuistriatus*.

A Coniacian assemblage consisting of *Mesopuzosia yubarensis*, *Nipponites baccus*, *Damesites* aff. *sugata*, and *Inoceramus uwajimensis* is abundant in the upper middle part of the Bykov Formation (Fig. 2). *Jimboiceras mihoense*, which is indicative of the Upper Coniacian in Hokkaido, also occurs in the middle part of the formation.

The first appearance datum of *Sphenoceramus naumanni*, *Inoceramus amakusensis*, *Gaudryceras tenuiliratum*, and *Yokoyamaoceras ishikawai*, indicating a Santonian age (Maeda, 1993), is in the upper part of the Bykov Formation exposed along the Krasnoyarka and Seim Rivers (Figs. 1, 2). This Santonian fauna is abundant throughout the upper part of the formation except in the uppermost part. *Gaudryceras* spp. are especially abundant in a stratigraphically limited (<100 m) interval providing a practical biozone for local correlation (herein named the *Gaudryceras* spp. acme zone; Fig. 2).

The basal sandy mudstone of the overlying Krasnoyarka Formation yields numerous *Eupachydiscus haradai*, which are most abundant in the Lower Campanian in Hokkaido. The succeeding bedded sandstone is extremely rich in *Sphenoceramus schmidti*, a diagnostic species of the Lower Campanian. Abundant occurrence of *Canadoceras kossmati* in the lower part of the Krasnoyarka Formation also suggests a late Early Campanian age (Zakharov et al., 1984; Toshimitsu et al., 1995). A Late Campanian age is characterized by abundant occurrence of *Canadoceras multicostatum*, '*Pachydiscus*' *soyaensis*, and an associated fauna (Matsumoto, 1984).

A Maastrichtian ammonoid assemblage characterized by *Pachydiscus subcompressus*, *Anagaudryceras matsumotoi*, and *Zelandites varuna* is predominant in the middle siltstone member of the Krasnoyarka Formation (Fig. 2). Therefore, the Campanian–Maastrichtian boundary probably lies in the sandstone unit just below this mudstone member.

The last occurrence of ammonoids is within the uppermost part of the middle siltstone member. Neither ammonoids nor inoceramids were recovered from the units above.

Recently, Kodama et al. (2000, 2002) established a magnetostratigraphy for the upper Bykov and Krasnoyarka Formations using the same outcrop sections (Krasnoyarka River and Seim River sections) as this study. They recognized nine chrons, namely C34n to C30n in these formations. Their chronology assigned the Santonian–Campanian boundary at the base of C33r in the upper part of the Bykov Formation. This horizon is located biostratigraphically in the middle of the *Gaudryceras* spp. acme zone (Fig. 2). The Campanian–Maastrichtian boundary is located in the

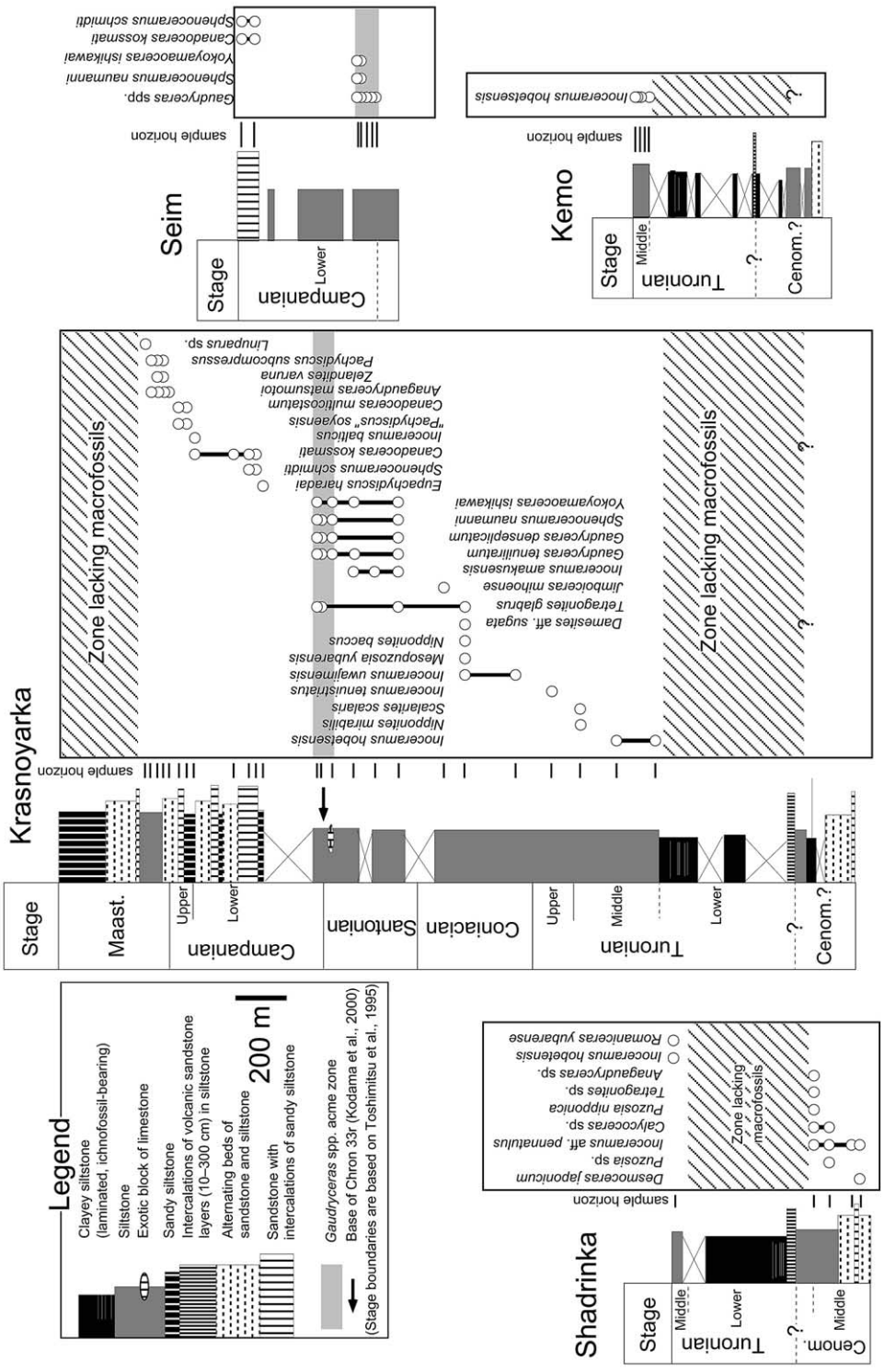

Fig. 2. Geologic columns showing lithology and distribution of representative macrofossil species along the Shadrinka, Krasnoyarka, Seim and Kemo River sections. Note two stratigraphic ranges from which no macrofossil occurs (zones lacking macrofossils).

Table 1
Carbon isotopic ratio of the Krasnoyarka River section

Sample	Sample horizon	$\delta^{13}C$ vs. PDB (‰)	C_{org} (%)
NIB-114	175	−23.16	0.40
NIB-113	185	−23.54	0.51
*NIB-112	210	−23.48	0.40
NIB-111	225	−23.80	0.44
*KRY-001	403	−24.35	0.49
KRY-002	415	−24.18	0.33
*KRY-112	463	−24.24	0.34
KRY-003	490	−24.59	0.51
*KRY-113	513	−24.57	0.44
KRY-004	551	−24.02	0.43
*KRY-005	606	−24.70	0.49
KRY-006	670	−24.56	0.64
*KRY-114	738	−24.78	0.61
KRY-115	783	−24.53	0.44
*KRY-008	800	−24.84	0.46
KRY-009	862	−24.76	0.56
*KRY-010	891	−24.28	0.48
KRY-011	923	−24.39	0.45
*KRY-012	960	−24.26	0.65
KRY-116	1004	−24.13	0.67
*KRY-117	1032	−24.07	0.59
KRY-013	1083	−24.18	0.58
*KRY-118	1108	−23.92	0.63
KRY-014	1134	−24.70	0.68
KRY-119	1173	−23.92	0.59
KRY-015	1231	−24.23	0.55
KRY-120	1287	−23.93	0.56
*KRY-018	1364	−24.11	0.52
KRY-019	1406	−24.07	0.91
*KRY-020	1440	−24.18	0.62
*KRY-121	1593	−24.40	0.66
KRY-021	1621	−24.21	0.57
KRY-022	1649	−23.90	0.51
*KRY-023	1674	−23.64	0.56
*KRY-024	1825	−23.63	0.69
KRY-122	1871	−23.89	0.63
*KRY-123	1882	−23.46	0.55
*KRY-025	1886	−23.76	0.76
KRY-124	1904	−23.78	0.59
KRY-125	1944	−23.71	0.65
*KRY-137	2161	−23.94	0.81
KRY-136	2176		0.11
*KRY-135	2188	−25.15	0.46
KRY-134	2208	−24.99	0.27
KRY-133	2246	−25.60	0.12
KRY-132	2273	−25.59	0.15
KRY-027	2302	−24.85	0.27
*KRY-028	2319	−25.56	0.13
KRY-131	2389	−24.93	0.57
KRY-029	2396	−25.15	0.14
KRY-130	2423	−25.07	0.57
KRY-030	2430	−25.01	0.71
KRY-035	2433	−25.22	0.59
KRY-129	2436	−25.39	0.62
KRY-031	2447	−25.38	0.49
*KRY-032	2455	−25.13	0.44
KRY-033	2470	−25.07	0.27
KRY-128	2491		0.03
*KRY-127	2514	−25.51	0.35
KRY-126	2537	−25.05	0.09
KRY-101	2581	−25.68	0.33
KRY-040	2581	−25.43	0.39
KRY-102	2599	−25.70	0.37
*KRY-039	2602	−25.65	0.41
*KRY-041	2619	−25.43	0.48
*KRY-105	2637	−25.60	0.30
KRY-109	2651	−25.72	0.47
KRY-108	2658	−25.77	0.44
KRY-104	2661	−25.26	0.09
KRY-043	2675	−24.90	0.64
KRY-106	2741	−24.44	0.30
*KRY-107	2815	−24.24	0.53
KRY-045	2828	−24.18	0.31
KRY-110	2848	−24.31	0.61
KRY-111	2863	−24.55	0.47
KRY-046	2908	−24.36	0.53
*KRY-047	2964	−24.31	0.37

Samples with asterisk on the head were performed in a petrographic study to certify predominant terrestrial origin of organic matter. Sample horizon is indicated stratigraphically by vertical separation from the upper limit of 'Shadrinka Sandstone' in the lower Bykov Formation.

middle of the Krasnoyarka Formation based on subchrons in C32n. The chronostratigraphic framework based on magnetostratigraphy is in good agreement with the molluscan biochronology.

4. Methods and materials

Samples were collected from natural outcrops along the Shadrinka, Naiba, Krasnoyarka, Kemo and Seim Rivers in the Naiba area (Fig. 1; Tables 1–4). All samples used for isotopic analysis were obtained from the mudstone unit with a sampling interval of 50 m or less when continuous exposure was available. The section along the Krasnoyarka River covers the Middle Cenoma-

Table 2
Carbon isotopic ratio of the Kemo River section

Sample	Sample horizon	$\delta^{13}C$ vs. PDB (‰)	C_{org} (%)
*KMO-005	−130	−22.85	0.30
KMO-004	−112	−23.41	0.34
KMO-003	4	−23.95	0.54
*KMO-002	225	−23.91	0.44
*NIB-010	277	−24.26	0.40
NIB-009	286	−24.29	0.51
NIB-008	295	−24.31	0.49
NIB-007	313	−24.53	0.50
*NIB-006	326	−24.78	0.35
KMO-001	346	−24.69	0.40

See caption of Table 1.

Table 4
Carbon isotopic ratio of the Seim River section

Sample	Sample horizon	$\delta^{13}C$ vs. PDB (‰)	C_{org} (%)
SEM-001	−533	−23.94	0.72
SEM-002	−485	−24.05	0.67
SEM-003	−450	−24.01	0.72
SEM-004	−399	−24.07	0.70
*SEM-005	−394	−23.94	0.64
SEM-006	−327	−24.28	0.74
SEM-007	−239	−24.34	0.76
SEM-008	−172	−24.39	0.74
*SEM-009	−48	−24.17	0.83
*SEM-101	27	−24.84	0.63
*SEM-104	84	−25.19	0.46

See caption of Table 1.

nian to Maastrichtian offering the principal section for this study. Because some stratigraphic intervals are not exposed or deeply weathered, three additional sections are used for the composite section. The sections are lithologically and biostratigraphically well correlated allowing construction of a composite section (Fig. 3). For correlation between the Shadrinka, Kemo and the Krasnoyarka River sections, two distinct lithological horizons and the first occurrence of *Inoceramus hobetsensis* were employed. The biostratigraphic horizon almost corresponds to the lithological boundary that separates siltstone from the underlying laminated clayey siltstone. Between the Seim and Krasnoyarka sections, the lithological boundary between the Bykov and Krasnoyarka Formations and the biostratigraphic acme zone of *Gaudryceras* spp. are employed for correlation.

Table 3
Carbon isotopic ratio of the Shadrinca River section

Sample	Sample horizon	$\delta^{13}C$ vs. PDB (‰)	C_{org} (%)
NFT-004	−267	−23.97	0.47
*NFT-005	−170	−23.54	0.30
NFT-006	−109	−23.65	0.39
NFT-007	−84	−24.20	0.29
*NFT-008	−68	−22.71	0.40
NFT-009	6	−23.60	0.14
*NFT-010	95	−23.52	0.38
*NFT-108	132	−23.45	0.33
NFT-107	142	−23.59	0.50
*NFT-106	180	−23.95	0.46
NFT-105	195	−23.45	0.27
*NFT-104	220	−23.98	0.39
NFT-103	249	−23.78	0.42
*NFT-102	317	−23.90	0.56
NFT-101	463	−24.61	0.39

See caption of Table 1.

Powdered mudstones were treated with a 5 N solution of HCl for 12 h to remove carbonate minerals. After repeated rinsing with deionized water to remove Cl^-, each neutralized sample was dried and sealed in a tube under vacuum together with CuO and then baked in an oven at 850°C for 8 h to convert organic carbon into CO_2 gas. After purification of CO_2 gas on a cryogenic vacuum line, carbon isotope analyses were performed with a Finnigan MAT delta-E mass spectrometer in the Biogeochemical Laboratories at Indiana University. The results reported herein are obtained using reference CO_2 calibrated by NBS standards. All isotopic values are expressed in the standard delta notation with respect to the PDB standard, where $\delta^{13}C = \{(^{13}C/^{12}C)_{sample}/(^{13}C/^{12}C)_{standard} - 1\} \times 1000$. The isotopic values were checked by an isotopically well-characterized laboratory standard (triphenylamine). Repeated analysis of the laboratory standard indicates a carbon isotope value with a reproducibility of ±0.2‰. Total organic carbon content (C_{org}) of whole rock was defined from CO_2 gas volume measured with a Baratron pressure transducer.

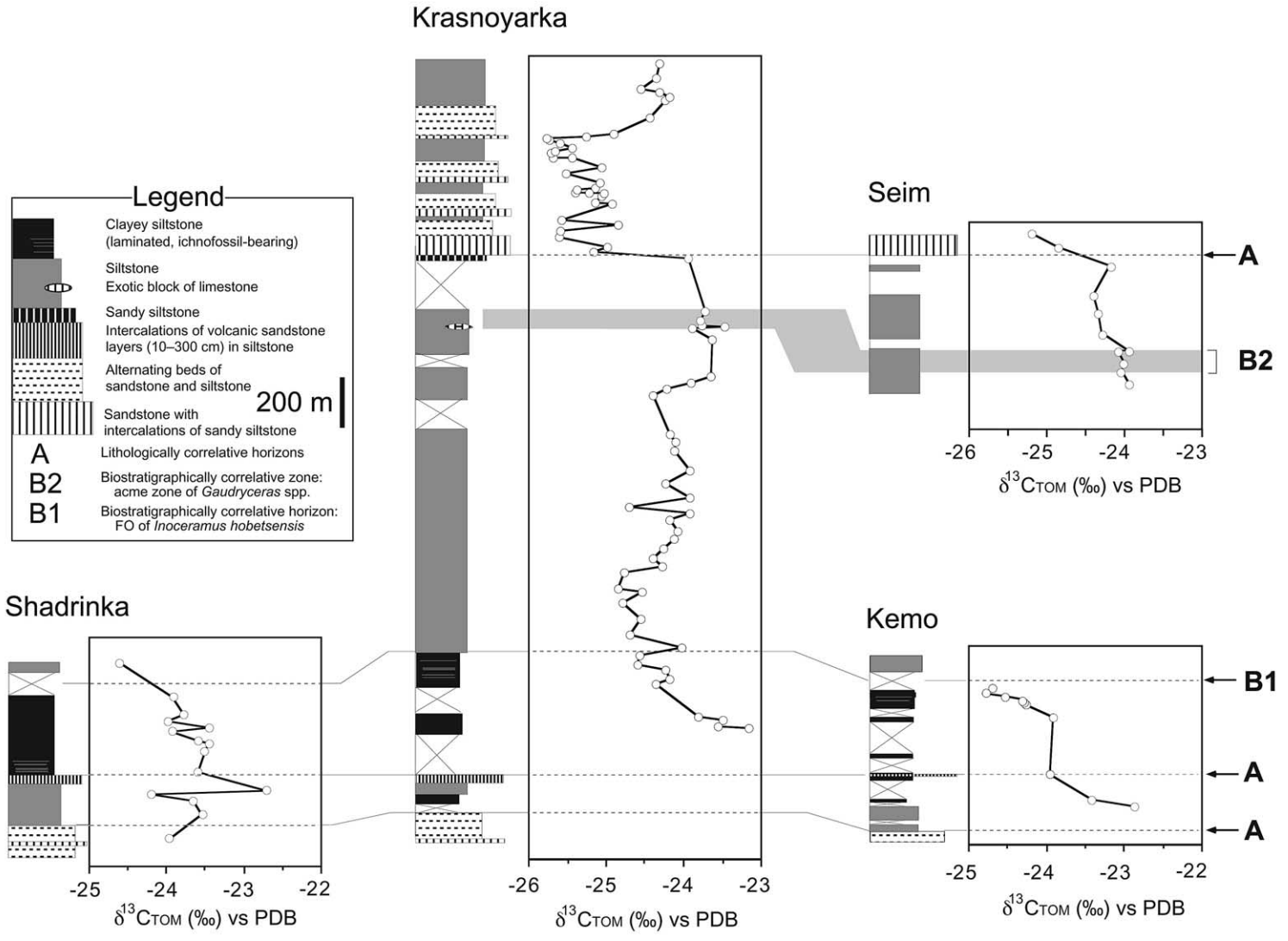

Fig. 3. Geologic columns and stratigraphic fluctuations of $\delta^{13}C$ of TOM along the Shadrinka, Krasnoyarka, Seim and Kemo River sections. Two biostratigraphic (B1, B2) and three lithostratigraphic (A) markers are employed to correlate them in order to construct a composite section.

Organic compositions of mudstone samples collected for carbon isotope analysis were checked by visual observation of kerogen. Crushed mudstone was made into polished blocks following the standard preparation procedure (Bustin et al., 1983). Polished pellets were examined using a MPV-2 microscope to identify organic particles.

5. Property of organic matter

Kerogen in selected samples was identified optically under reflected light and in fluorescent mode. Microscopic observations were carried out on 43 selected samples (Table 1–4) covering all major isotopic events through the studied sections. Kerogen from all selected samples is dominated by vitrinite, inertinite (fusinite and semifusinite) and equivalent small particles namely vitrodetrinite and inertodetrinite. This suite of kerogen types is derived exclusively from cellular lignins of terrestrial vascular plants. Preservation of cell structure in semifusinite indicates its origin as woody plant matter. Organic matter other than terrestrial woody plant (e.g. alginite and liptinite) was rarely ($\ll 1\%$) detected during microscopic examination. Sporinites, resinites and bitumen constitute the only fluorescent organic matter in the samples. This limited fluorescent property is best explained by an absence of marine organic matter. Some non-oxidized vitrinite could have incorporated marine organic molecules through the process of condensation during early stage of diagenesis. But in such a case, marine alginite and/or liptinite should have been a more conspicuous component under the microscope. The result of visual observation of kerogens strongly suggests that no significant marine organic materials have been incorporated in the kerogens. A part of the result has been published and discussed in a previous paper (Hasegawa, 2001). These characteristics of organic carbon from the Middle Cenomanian–Maastrichtian sediments of Naiba area are nearly identical with those from the Cenomanian–Turonian sections from the Oyubari and Kotanbetsu areas in Hokkaido, Japan (Hasegawa, 1997, 2001; Hasegawa and Hatsugai, 2000).

6. Time-stratigraphic fluctuations of $\delta^{13}C$ and C_{org} through the Upper Cretaceous

Stratigraphic profiles of $\delta^{13}C$ for the Shadrinka River, Krasnoyarka River, Kemo River and Seim River sections are shown in Fig. 3. The isotopic data were re-plotted on the composite section (referred to 'Naiba section' later; Fig. 4) based on correlations shown in Fig. 3. Stratigraphic fluctuations in the isotopic ratio of terrestrial organic carbon from the Middle Cenomanian to the Maastrichtian of the Naiba section exhibit distinctive characters (Fig. 4), allowing separation into 13 segments (NB0–NB12).

Segment NB0 is represented by four sample points from the Shadrinka River section showing a modest positive excursion (~ -24 to $\sim -23.5‰$) in the middle of the Middle Cenomanian and a negative shift ($\sim -24.2‰$) above the last occurrence of Cenomanian macrofossils. The globally recognized carbon isotopic 'spike' across the Cenomanian–Turonian (C–T) boundary is observed in both the Shadrinka River and Kemo River sections (NB1), with a peak value of $-22.7‰$. Just above the C–T spike, a single point separating NB2 from NB1 shows a sharp break ($\sim -24‰$). A step-like ($\sim -23.5‰$), relatively stable segment with a faint peak near the top (NB2) is followed by a segment with a negative shift (NB3). At the top of NB3, there is a positive outstanding point ($\sim 0.5‰$ spike). NB2 is defined by samples from the Shadrinka River section and NB3 from the Shadrinka River, Kemo River and Krasnoyarka River sections. The interval from NB1 through NB3 nearly corresponds to the 'zone lacking macrofossils'. Relatively stable values persist ($\sim -24.7‰$) through the Middle Turonian (NB4), followed by a positive shift to a broad plateau (NB5: $\sim -23.9‰$) through the Coniacian with a distinctive negative peak (one point) near the Turonian–Coniacian boundary. This segment encompasses the *Inoceramus uwajimensis* zone (Toshimitsu et al., 1995). Above this NB5 plateau, isotopic values shift positively to $\sim -23.5‰$ (NB6) which is the maximum value of the section above the Middle Turonian. The NB6 maximum is located just below the Santonian–Campanian boundary, coincident with the

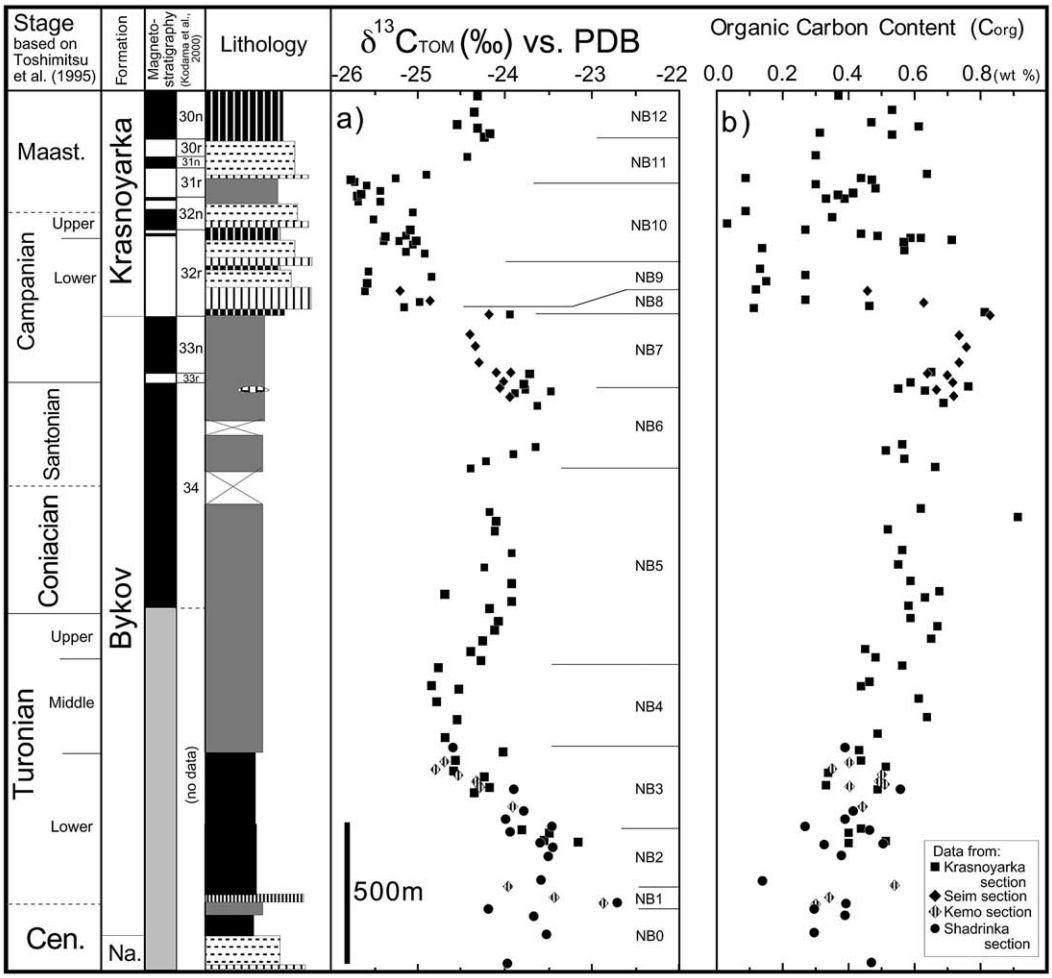

Fig. 4. Carbon isotope stratigraphy of TOM, and fluctuation of C_{org} through the composite Naiba section. Magnetostratigraphy by Kodama et al. (2000) is also indicated. The $\delta^{13}C$ profile can be divided into 13 segments (NB0–NB12). Note most $\delta^{13}C$-positive horizon (NB2) near the C/T boundary and most negative horizon (top of NB10) in C33r near the bottom of the Maastrichtian. The $\delta^{13}C$ shows dramatic negative shift at the lithological boundary between the Bykov and Krasnoyarka Formations. The fluctuation of C_{org} also shows conspicuous turnover of its phase at this lithologic boundary. See Figs. 2 or 3 for legend.

base of C33r. The stratigraphic range of NB6 is almost equivalent to the Santonian *Inoceramus amakusensis* zone (Toshimitsu et al., 1995). NB4–NB7 are defined by samples from the Krasnoyarka River section. Above the Santonian–Campanian boundary, the carbon isotopic curve shows a brief trough (NB7) having a minimum value of ~ -24.3‰ through C33r and C33n in the lower part of the Lower Campanian. NB7 is only documented from the Seim River section. The time-stratigraphic pattern for C_{org} shows a consistent increase from $\sim 0.3\%$ to $\sim 0.8\%$ from the Middle Cenomanian to the Lower Campanian Bykov Formation (Fig. 4). At the boundary between Bykov and Krasnoyarka Formations in the Lower Campanian, a marked negative shift (NB8) of the $\delta^{13}C$ value is documented in both the Krasnoyarka River and Seim River sections. The first negative shift of C_{org} coincided with the distinct lithological changes exhibits a remarkable inflection of the C_{org} curve (Fig. 4). Above the NB8 shift, $\delta^{13}C$ values become unstable and oscillate

between −24.8‰ and −25.6‰ through NB9 in the lower part of the Lower Campanian Krasnoyarka Formation. A similar oscillatory feature is more obvious in the C_{org} profile. A major turnover in C_{org} occurs at the Bykov–Krasnoyarka Formation boundary, changing from an increasing trend with smaller (generally $<0.3\%$) variation below into larger (0.03–0.8%) variation with no increasing/decreasing trend above. The $\delta^{13}C$ curve shows a negative shift (NB10) through the upper part of Lower Campanian, Upper Campanian and the bottom of the Maastrichtian. The $\delta^{13}C$ value of −25.8‰ in C31r, the lower part of Maastrichtian, is the most negative value within the Naiba section. This negative point corresponds to the last occurrence of macrofossils in this section. Higher in the section, the $\delta^{13}C$ values fluctuate but there is a sharp positive rebound (NB11) through the upper part of C31r, 30n and 30r, and reach ∼−24.2‰ near the top of C30r. Values of $\delta^{13}C$ are stable (NB12) through C30n toward the top of the Naiba section. Isotopic segments NB9–NB12 are only observed in the Krasnoyarka River section.

7. Correlation between carbon isotopic curves of TOM and carbonate

Carbon isotopic fluctuations of the TOM from the Naiba section through the Cenomanian and Turonian are well correlated to those from the Oyubari (Hasegawa, 1997) and Tappu (Hasegawa and Saito, 1993; Hasegawa, 1994) sections in Japan (Fig. 5). Hasegawa and Hatsugai (2000) documented that the global Middle Cenomanian positive excursion and following 'non-global' Upper Cenomanian negative excursion in the $\delta^{13}C$ profiles of TOM could be correlated between the Kotanbetsu and Oyubari sections. In the Naiba section, these isotopic events are not clearly recognized because of low stratigraphic resolution in this time interval; however, there appears to be a positive excursion in the middle of NB0, and a following negative excursion (only one data point) just below NB1 (Fig. 5).

Segments NB1–NB4 are observed in the Oyubari (Fig. 5; Hasegawa, 1997) and Kotanbetsu (Hasegawa and Hatsugai, 2000) sections. Segments NB1–NB3 are also recognized in the Tappu section (Fig. 5; Hasegawa and Saito, 1993; Hasegawa, 1994). The magnitude of the $\delta^{13}C$ fluctuations and the $\delta^{13}C$ values observed in each isotopic segment are similar to those of correlative segments in Japanese sections, except for NB1. The magnitude of the isotopic spike in NB1 in the Naiba section is >0.6‰ smaller than that of Japanese sections. Sparse sampling and less exposure of outcrops across the Cenomanian–Turonian boundary in the Naiba section are probably the reason for this difference in magnitude. A negative break (just one point) between NB1 and NB2 can also be correlated to the Tappu and Oyubari sections (Fig. 5).

Carbon isotopic stratigraphy of Upper Cretaceous marine carbonates has been well studied in Europe (e.g. Corfield et al., 1991; Jenkyns et al., 1994; Stoll and Schrag, 2000) and North America (e.g. Pratt, 1985; Hayes et al., 1989; Pratt et al., 1993). For the Campanian and Maastrichtian, ODP 690C from the South Atlantic Ocean provides a detailed carbon isotopic stratigraphy, which is age-controlled by magnetostratigraphy (Barrera and Huber, 1990). Barrera and Savin (1999) noted that the generally similar $\delta^{13}C$ curves from the South Atlantic, North Atlantic, Indian Ocean and Tropical Pacific through this time interval permit the use of $\delta^{13}C$ patterns to 'fine-tune age assignments'. The comparison between the $\delta^{13}C$ curves of the carbonate and TOM is shown in Fig. 5. General features of the patterns are well correlated between the marine carbonate and the TOM. The isotopic segments correlative to NB1–NB6 and lower half of NB7 are clearly observed in the Western Interior sections (Hayes et al., 1989; Pratt et al., 1993) and the South England section (Jenkyns et al., 1994) with similar magnitudes of fluctuations. Even a small spike at the top of the NB3 (Turonian) is correlative to the South England section. This small peak has been employed for high-resolution chemostratigraphic correlation in Central and Western Europe (Voigt and Wiese, 2000). Although the overall magnitude appears to be depressed, presumably because of diagenesis, the Bottaccione Gorge section, Italy (Fig. 5; Corfield

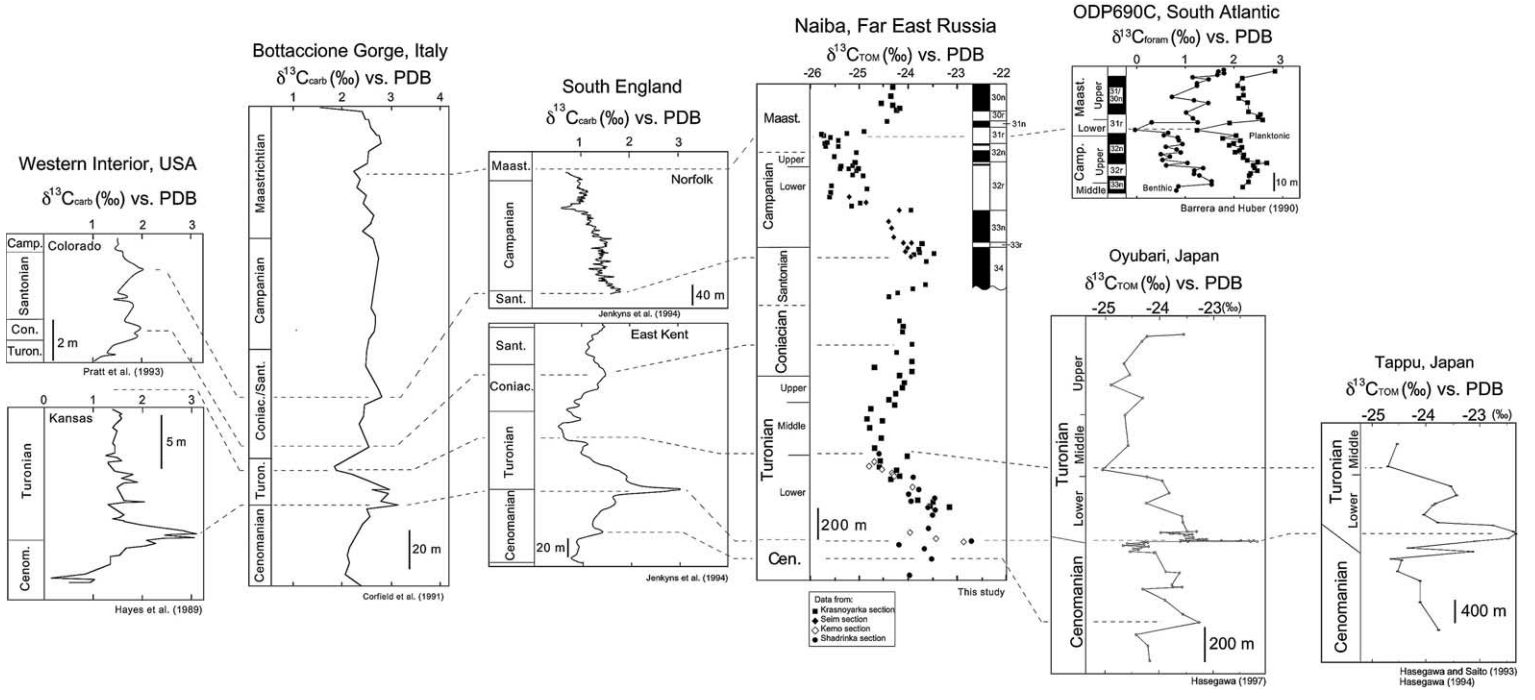

Fig. 5. Comparison of carbon isotope profiles for carbonate and TOM. Correlative $\delta^{13}C$ events are connected with broken lines. Note nearly parallel fluctuations with similar amplitude between the TOM from the Naiba section and the carbonate from the South England section through the uppermost Cenomanian–lower part of Lower Campanian. $\delta^{13}C_{carb}$: carbon isotope ratio for carbonate; $\delta^{13}C_{TOM}$: carbon isotope ratio for TOM; $\delta^{13}C_{foram}$: carbon isotope ratio for foraminifers.

et al., 1991) shows similar $\delta^{13}C$ fluctuations to the Naiba section. Jenkyns et al. (1994) and Stoll and Schrag (2000) have reported similar $\delta^{13}C$ feature from this and related sections around Gubbio, Italy. The isotopic segments NB7 (upper half), NB10, NB11 and NB12 are also well identified in the $\delta^{13}C$ curves of ODP 690C obtained from planktonic and benthic foraminifers (Fig. 5; Barrera and Huber, 1990). ODP 690C is well age-controlled by magnetostratigraphy as is the Naiba section. The most negative value of the Naiba section at the top of NB10 can be correlated to the Middle Maastrichtian trough in the Bottaccione Gorge section and to the horizon above the top of the Norfolk section (Fig. 5). The negative excursion observed in the upper Campanian of the Norfolk section could not be distinguished in the Naiba section presumably because of the stratigraphic missing or condensation. The isotopic features of NB8 and NB9 in C32R of the Naiba section are not recognized in any of the currently published isotopic curves for carbonate (see Fig. 5 for South Atlantic as an example). The larger magnitude of the shift (1–1.5‰) for NB8 cannot be compared to the smaller negative excursion observed in the Upper Campanian of the Norfolk section in South England (Fig. 5).

8. Factors controlling $\delta^{13}C$ value

There are two different types of factors that influence the $\delta^{13}C$ value for TOM. One type is a set of factors that affect both $\delta^{13}C$ values for marine carbonate and TOM (Type-A factors), leading to coupled $\delta^{13}C$ fluctuations. Another type is a set of factors that affect only $\delta^{13}C$ values for TOM (Type-B factors) leading to decoupled $\delta^{13}C$ curves of TOM and marine carbonate.

Diagenesis of TOM would change the $\delta^{13}C$ value, causing degraded TOM to have a different $\delta^{13}C$ value than originally buried TOM. One effective factor that alters organic properties during diagenesis is thermal maturation. But it is unlikely that only a few horizons have been thermally matured leading to the substantial $\delta^{13}C$ events. Selective decomposition of TOM (preferential decomposition of cellulose against lignitic material) would have occurred during early diagenesis (Benner et al., 1987); however, preserved material observed in this study is exclusively lignitic in origin and probably resistant to further diagenesis. Organic matter in the studied sections that was solubilizable during early diagenesis was entirely removed and has not caused carbon isotopic fractionation for preserved organic matter. Bocherens et al. (1994) showed only small intraspecific variation of $\delta^{13}C$ (between −26.6 and −25.4‰) in Late Triassic fossil plants from eight different localities, suggesting that isotopic alteration by diagenesis is not an important factor for $\delta^{13}C$ study of lignitic TOM. It is interpreted that diagenesis is an insignificant or minor factor for stratigraphic fluctuation of the $\delta^{13}C$ value in this study.

8.1. Coupled isotopic shifts in marine carbonate and TOM (Type-A factors)

Parallel fluctuations and similar magnitudes of the isotopic events in the $\delta^{13}C$ curves from both TOM and marine carbonate suggest that the carbon isotopic fluctuations identified as NB1–NB7 were controlled by the Type-A factors. The likely linkage for the Type-A factors is a $\delta^{13}C$ fluctuation of CO_2 in the global ocean-atmospheric reservoir. NB10–NB12 are also interpreted to be controlled mainly by Type-A factors; however, variable lithology and sample-to-sample variation of the C_{org} (Fig. 4) suggest minor local perturbations related to Type-B factors and/or small gaps in the stratigraphic section.

8.2. Decoupled $\delta^{13}C$ shifts in marine carbonate and TOM (Type-B factors)

There is a clear dependence between an isotopic shift at NB8 and lithology. The shift is coincident with the formation boundary between the Bykov and Krasnoyarka Formations and represents a provenance and depositional shift from slope basin to deltaic environments. NB8 may be linked to a turnover in the provenance of TOM, whereas NB9 in the Krasnoyarka Formation may reflect more local variability than the isotopic features in the Bykov Formation. Type-B factors may have

superimposed additional features on a $\delta^{13}C$ curve of TOM resulting from Type-A factor. Arens et al. (2000) compiled diverse factors influencing carbon isotopic discrimination in C3 land plants. Some of these factors could have acted as Type-B factors for TOM. TOM in the Naiba samples is interpreted to be generally well mixed during transportation from its provenance to depositional site. Additional mixing resulted from post-depositional bioturbation. Factors like low light, osmotic stress, low nutrients, age (juvenile vs. adult), sun vs. shade leaves, and seasonal variation are largely eliminated by mixing and, therefore, are interpreted to be too local or too short in duration to act as primary factors on fluctuating the $\delta^{13}C$ value in the Naiba section. Low temperature (polar regions during ice-house time) is probably not a primary factor since the sedimentary basin for the Naiba section was located at more or less the same latitude as present (Kodama et al., 2000). Reasonable Type-B factors for TOM in this study are: (a) recycled CO_2 (closed or open forest); (b) water stress, low relative humidity; (c) reduced pCO_2 with altitude; and (d) growth form and deciduousness (taxonomic composition of plant community). These factors are geography dependent and may be linked to the turnover in provenance for terrestrial detritus that caused a lithology-dependent negative shift of the $\delta^{13}C$ value (NB8). The $\delta^{13}C$ fluctuation expressed as NB9 in the Krasnoyarka Formation is interpreted to reflect an exaggeration of local variation in these Type-B factors associated with a lateral facies shift in a deltaic environment. Sample-to-sample variation of the $\delta^{13}C$ value is not conspicuous above NB9, whereas C_{org} fluctuates prominently in NB10 and NB11. It is inferred that local sedimentary processes also influenced NB10 and NB11 causing some superimposed local noise on the $\delta^{13}C$ curve.

Type-B factors also are interpreted to have controlled the negative shift in NB0 and the negative break at the NB1–NB2 boundary. These events are located just below and above the C–T boundary excursion (NB1). Correlative isotopic events are observed in TOM from Hokkaido sections (Fig. 5; see also Hasegawa and Hatsugai, 2000 for the Kotanbetsu section), although no similar features are reported from any carbonate sections. Hasegawa (in press) discussed this phenomenon in detail.

9. Paleoatmospheric CO_2 and coupled $\delta^{13}C$ fluctuation between TOM and carbonate

Enhanced carbon flux from oceanic reservoir to sedimentary organic carbon (increased rate of organic carbon burial) can selectively withdraw ^{12}C relative to ^{13}C leading to a more positive $\delta^{13}C$ value for the ocean-atmospheric CO_2 reservoir (e.g. Scholle and Arthur, 1980; Arthur et al., 1987; Jenkyns et al., 1994). If a positive shift of the $\delta^{13}C$ value of marine carbonate is ascribed to an isotopic shift of the oceanic reservoir, then a coincidental lowering of ocean-atmospheric pCO_2 should be involved. Lowering pCO_2 results in a reduction of carbon isotopic fractionation during photosynthesis leading to an enhanced positive $\delta^{13}C$ shift in MOM (Arthur et al., 1988; Popp et al., 1989; Hollander and Mckenzie, 1991; Hayes, 1993; Hayes et al., 1999; Kump and Arthur, 1999; Panagi et al., 1999) but does not enhance the $\delta^{13}C$ shift in marine carbonate. An opposite effect is expected when organic matter previously deposited in a sedimentary basin is exposed and oxidized, leading to a negative isotopic shift and increase in pCO_2 of the ocean–atmosphere system (Arthur et al., 1988). Therefore, $\delta^{13}C$ values of MOM reflect $\delta^{13}C$ fluctuations of the ocean-atmospheric reservoir *and* a superimposed pCO_2-related enhancement. As a result, $\delta^{13}C$ values of MOM tend to show greater fluctuations than associated fluctuations in marine carbonate. A debate continues about whether the long-term record of TOM is affected by atmospheric pCO_2 in a manner similar to MOM. Popp et al. (1989) discussed stomatal regulations (density and conductance) in connection with water transpiration that can offset the pCO_2 effect and stabilize carbon isotopic fractionation in C3 plants. On the other hand, Gröcke et al. (1999) documented an exaggerated $\delta^{13}C$ fluctuation in TOM for Barremian through Albian strata and interpreted pCO_2 and isotopic composition of atmospheric CO_2 as acting together to produce an

enhanced fluctuation. The magnitude of fluctuation reported by Gröcke et al. (1999) is conspicuously similar to that of the MOM from the same time period (Menegatti et al., 1998). Therefore, a pCO_2 factor cannot be excluded from potential factors enhancing $\delta^{13}C$ fluctuations for TOM compared to marine carbonate. Alternatively, the atmospheric pCO_2-linked modification of the paleoclimate and/or complex terrestrial ecosystem might have emphasized Type-B factors (e.g. humidity) coincident with Type-A factor-induced fluctuations of $\delta^{13}C$ leading to exaggerated $\delta^{13}C$ fluctuations in TOM as reported by Gröcke et al. (1999).

In contrast to enhanced shifts in organic matter, diagenetically altered marine carbonate tends to yield diminished $\delta^{13}C$ fluctuations. During diagenesis, carbonate can experience repetitive dissolution and recrystallization leading to a stratigraphically smoothed $\delta^{13}C$ profile. The Bottaccione Gorge (Fig. 5; Corfield et al., 1991) and other sections near Gubbio, Italy (Jenkyns et al., 1994; Stoll and Schrag, 2000) are interpreted to be diagenetically smoothed. An example of a chalk section with original $\delta^{13}C$ values preserved in carbonate is the South England section (Fig. 5; Jenkyns et al., 1994). Preservation of near-primary $\delta^{18}O$ values, which are more susceptible to diagenetic alteration than are $\delta^{13}C$ values, signifies unaltered $\delta^{13}C$ fluctuations (Jenkyns et al., 1994).

Parallel fluctuations of $\delta^{13}C$ values and similar magnitudes are observed for TOM from the Naiba section, and marine carbonate from South England and the U.S. Western Interior for uppermost Cenomanian through Lower Campanian strata (Fig. 5). This coordinated isotopic behavior suggests that (1) the $\delta^{13}C$ profile of TOM from the Naiba section is at minimum enhanced by pCO_2, that (2) the $\delta^{13}C$ profiles of marine carbonates from South England (Jenkyns et al., 1994) and U.S. Western Interior (Hayes et al., 1989; Pratt et al., 1993) are little altered by diagenesis, and that (3) carbon isotopic equilibrium was reached between surface ocean and atmosphere during this period. Consequently, the $\delta^{13}C$ curve for TOM from the Naiba section can be a proxy for the carbon isotopic composition of paleoatmospheric CO_2 during the Late Cenomanian through Early Campanian, offering an important reference section for the carbon isotope stratigraphy for this critical interval of global transition from a warming to a cooling climate.

10. Conclusion

The carbon isotope stratigraphy of organic matter through the Middle Cenomanian–Maastrichtian was studied in the Naiba area, Sakhalin Island, Far East Russia. A petrographic study demonstrates that the preserved organic matter is almost exclusively terrestrial. The time-stratigraphic profile of the $\delta^{13}C$ fluctuations are compared with previous studies on marine carbonate carbon. The salient conclusions are as follows:

(1) General features of the carbon isotope profiles are well correlated between marine carbonate and terrestrial organic matter using macrofossil biostratigraphy and magnetostratigraphy.

(2) A $\delta^{13}C$ fluctuation of CO_2 in the global ocean-atmospheric reservoir is the primary factor influencing the coupled isotopic shifts in marine carbonate and terrestrial organic matter observed in uppermost Cenomanian through Lower Campanian (segments NB1–NB7). The same primary factor caused fluctuation of the $\delta^{13}C$ in segments NB10–NB12; however, minor regional or local factors also are involved.

(3) The $\delta^{13}C$ curve for the uppermost Cenomanian through Lower Campanian from Sakhalin contains minimum superimposed signals on the $\delta^{13}C$ fluctuations of atmospheric CO_2. It is proposed as a proxy for the carbon isotopic composition of paleoatmospheric CO_2. The Naiba section offers an important reference for the carbon isotope stratigraphy for this time interval.

Acknowledgements

The authors express their deep appreciation to S. Studley and J. Fong of Indiana University for their technical support during analyses, and M. Mastalerz of the Indiana Geological Survey for her advice and helpful discussions during the

work on organic petrology. Acknowledgments are also due to K.F. Sergeev, the director of the Institute of Marine Geology and Geophysics, Yuzhno-Sakhalinsk, Y. Yan of and O. Melnikov of the same institute, G.S. Shteinberg, the director of the Institute of Volcanology and Geodynamics, Academy of Natural Sciences of the Russian Federation, Yuzhno-Sakhalinsk and A.V. Solov'yov of the same institute for their aids in obtaining permissions for the survey in Russia and for their assistance during the field survey. Financial support for this study was provided by the Postdoctoral Fellowships for Research Abroad program of Japan Society for the Promotion of Science (J.S.P.S.), a Grant-in-Aid for Encouragement of Young Scientists from the Government of Japan, no. 09740387, a Grant for Encouragement of Young Scientists from the Nissan Science Foundation (these three given to T.H.), and by Grant-in-Aid for International Scientific Research Program (Field Research) from the Government of Japan, nos. 05041068 (given to T.K.), 08041113 and 09041114 (given to K.U.).

References

Arens, N.C., Jahren, A.H., Amundson, R., 2000. Can C3 plants faithfully record the carbon isotopic composition of atmospheric carbon dioxide? Paleobiology 26, 137–164.

Arthur, M.A., Dean, W.E., Pratt, L.M., 1988. Geochemical and climatic effects of increased marine organic carbon burial at the Cenomanian/Turonian boundary. Nature 335, 714–717.

Arthur, M.A., Schlanger, S.O., Jenkyns, H.C., 1987. The Cenomanian–Turonian oceanic anoxic event, II. Paleoceanographic controls on Organic-matter production and preservation. In: Brooks, J., Fleet, A.J. (Eds.), Marine Petroleum Source Rocks. Geol. Soc. Spec. Publ. 26, pp. 401–420.

Barrera, E., Huber, B.T., 1990. Evolution of Antarctic waters during the Maastrichtian: Foraminifer oxygen and carbon isotope ratios, Leg. 113. Proc. ODP Sci. Res. 113, 813–827.

Barrera, E., Savin, S.M., 1999. Evolution of the late Campanian–Maastrichtian marine climates and oceans. In: Barrera, E., Johnson, C.C. (Eds.), Evolution of the Cretaceous Ocean–Climate System. Geol. Soc. Am. Spec. Pap. 332, pp. 245–282.

Benner, R., Fogel, M.L., Sprague, E.K., Hodson, R.E., 1987. Depletion of ^{13}C in lignin and its implications for stable carbon isotope studies. Nature 329, 708–710.

Bocherens, H., Friis, E.M., Mariotti, A., Pedersen, K.R., 1994. Carbon isotopic abundances in Mesozoic and Cenozoic fossil plants: Palaeoecological implication. Lethaia 26, 347–358.

Bustin, R.M., Cameron, A.R., Grieve, D.A., Kalkreuth, W.D., 1983. Coal Petrology, Its Principles, Methods, and Applications. Geol. Assoc. Canada Short Course Note vol. 3, Victoria, 230 pp.

Corfield, R.M., Cartlidge, J.E., Premoli-Silva, I., Housley, R.A., 1991. Oxygen and carbon isotope stratigraphy of the Paleogene and Cretaceous limestones in the Bottaccione Gorge and the Contessa Highway sections, Umbria, Italy. Terra Nova 3, 414–422.

Frakes, L.A., Francis, J.E., Syktus, J.I., 1992. Climate Modes of the Phanerozoic. Cambridge University Press, Cambridge, 277 pp.

Gröcke, D.R., Hesselbo, S.P., Jenkyns, H.C., 1999. Carbon isotope composition of Lower Cretaceous fossil wood: Ocean-atmosphere chemistry and relation to sea level change. Geology 27, 155–158.

Hasegawa, T., 1994. Cretaceous paleoenvironment across the Cenomanian/Turonian boundary based on analytical data from the Yezo Group, Hokkaido, Japan. D. Sci. Diss. Inst. Geol. Paleontol., Tohoku University, Sendai.

Hasegawa, T., 1995. Correlation of the Cenomanian/Turonian boundary between Japan and Western Interior of the United States. J. Geol. Soc. Japan 101, 2–12.

Hasegawa, T., 1997. Cenomanian–Turonian carbon isotope events recorded in terrestrial organic matter from northern Japan. Palaeogeogr. Palaeoclimatol. Palaeoecol. 130, 251–273.

Hasegawa, T., 2001. Predominance of terrigenous organic matter in Cretaceous marine fore-arc sediments, Japan and Far East Russia. Int. J. Coal Geol. 47, 207–221.

Hasegawa, T., in press. Cretaceous terrestrial paleoenvironments of northeastern Asia suggested from carbon isotope stratigraphy: Increased atmospheric pCO_2-induced climate. J. Asian Earth Sci.

Hasegawa, T., Hatsugai, T., 2000. Carbon-isotope stratigraphy and its chronostratigraphic significance for the Cretaceous Yezo Group, Kotanbetsu area, Hokkaido. Jpn. Paleontol. Res. 4, 95–106.

Hasegawa, T., Saito, T., 1993. Global synchroneity of a positive carbon isotope excursion at the Cenomanian/Turonian boundary: Validation by calcareous microfossil biostratigraphy of the Yezo Group, Hokkaido, Japan. Isl. Arc 2, 181–191.

Hayes, J.M., 1993. Factors controlling ^{13}C contents of sedimentary organic compounds: principle and evidence. Mar. Geol. 113, 111–125.

Hayes, J.M., Popp, B.N., Takigiku, R., Johnson, M.W., 1989. An isotopic study of biogeochemical relationships between carbonates and organic carbon in the Greenhorn Formation. Geochim. Cosmochim. Acta 53, 2961–2972.

Hayes, J.M., Strauss, H., Kaufman, A.J., 1999. The abundance of ^{13}C in marine organic matter and isotopic fractionation in the global biogeochemical cycle of carbon during the last 800 Ma. Chem. Geol. 161, 103–125.

Hollander, D.J., Mckenzie, J.A., 1991. CO_2 control on carbon-

isotope fractionation during aqueous photosynthesis: A paleo-pCO_2 barometer. Geology 19, 929–932.

Jenkyns, H.C., Gale, A.S., Corfield, R.M., 1994. Carbon- and oxygen-isotope stratigraphy of the English Chalk and Italian Scaglia and its palaeoclimatic significance. Geol. Mag. 131, 1–34.

Kaiho, K., Hasegawa, T., 1994. End-Cenomanian benthic foraminiferal extinctions and oceanic dysoxic events in the northwestern Pacific Ocean. Palaeogeogr. Palaeoclimatol. Palaeoecol. 111, 29–43.

Kodama, K., Maeda, H., Shigeta, Y., Kase, T., Takeuchi, T., 2000. Magnetostratigraphy of Upper Cretaceous strata in South Sakhalin, Russian Far East. Cretac. Res. 21, 469–478.

Kodama, K., Maeda, H., Shigeta, Y., Kase, T., Takeuchi, T., 2002. Integrated biostratigraphy and magnetostratigraphy of the upper Cretaceous system along the River Naiba in southern Sakhalin, Russia (in Japanese with English abstract). J. Geol. Soc. Japan 108, 366–384.

Kump, L.R., Arthur, M.A., 1999. Interpreting carbon-isotope excursions: carbonate and organic matter. Chem. Geol. 161, 181–198.

Kuypers, M.M.M., Pancost, R.D., Sinninghe Damsté, J.S., 1999. A large and abrupt fall in atmospheric CO_2 concentration during Cretaceous times. Nature 399, 342–345.

Laws, E.A., Popp, B.N., Bidigare, R.R., Kennicutt, M.C., Macko, S.A., 1995. Dependence of phytoplankton carbon isotopic composition on growth rate and $[CO_2]_{aq}$: Theoretical considerations and experimental results. Geochim. Cosmochim. Acta 59, 1131–1138.

Maeda, H., 1987. Taphonomy of ammonites from the Cretaceous Yezo Group in the Tappu area, northwestern Hokkaido, Japan. Trans. Proc. Palaeontol. Soc. Japan N.S. 148, 285–305.

Maeda, H., 1993. Dimorphism of the Late Cretaceous falsepuzosiine ammonites: Yokoyamaoceras Wright and Matsumoto, 1954 and Neopuzosia Matsumoto, 1954. Trans. Proc. Palaeontol. Soc. Japan N.S. 169, 97–128.

Matsumoto, T., 1942. Fundamentals in the Cretaceous stratigraphy of Japan, Part 1. Mem. Fac. Sci. Kyushu Imp. Univ. Ser. D 1, 129–280.

Matsumoto, T., 1954. The Cretaceous System in the Japanese Islands. Japanese Society for the Promotion of Science, Tokyo, 324 pp.

Matsumoto, T., 1959. Zonation of the Upper Cretaceous in Japan. Mem. Fac. Sci. Kyushu Univ. Ser. D 9, 55–93.

Matsumoto, T., 1977. Some heteromorph ammonites from the Cretaceous of Hokkaido. Mem. Fac. Sci. Kyushu Univ. Ser. D 23, 303–366.

Matsumoto, T., 1984. Some Ammonites from the Campanian (Upper Cretaceous) of northern Hokkaido. Palaeontol. Soc. Japan Spec. Pap. 27, 93 pp.

Matsumoto, T., Noda, M., Maiya, S., 1991. Towards an integrated ammonoid-, inoceramid-, and foraminiferal biostratigraphy of the Cenomanian and Turonian (Cretaceous) in Hokkaido. J. Geogr. 100, 378–398.

Matsumoto, T., Obata, I., Hirano, H., 1985. Mega-fossil zonation of the Cretaceous System in Japan and correlation with the standards in Western Europe (in Japanese). Mem. Geol. Soc. Japan 26, 29–42.

Menegatti, A.P., Weissert, H., Brown, R.S., Tyson, R.V., Farrimond, P., Strasser, A., Caron, M., 1998. High-resolution $\delta^{13}C$ stratigraphy through the early Aptian 'Livello Selli' of the Alpine Tethys. Paleoceanography 13, 530–545.

Mirolybov, Yu.G., 1987. Ammonites. In: Poyarkova, Z.N. (Ed.), Reference Section of Cretaceous Deposits in Sakhalin (Naiba Section). Trans. Acad. Sci. USSR, Leningrad 16, pp. 83–87 (in Russian).

Motoyama, I., Fujiwara, O., Kaiho, K., Murota, T., 1991. Lithostratigraphy and calcareous microfossil biostratigraphy of the Cretaceous strata in the Oyubari area, Hokkaido, Japan (in Japanese with English abstract). J. Geol. Soc. Japan 97, 507–527.

Okada, H., 1979. Geology of Hokkaido and plate tectonics (in Japanese). Earth (Chikyu) 1, 869–877.

Okada, H., 1983. Collision Orogenesis and Sedimentation in Hokkaido, Japan. In: Hashimoto, M., Uyeda, S. (Eds.), Accretion Tectonics in the Circum-Pacific Regions. Terra Scientific Publishing Company, Tokyo, pp. 91–105.

Panagi, M., Arthur, M.A., Freeman, K.H., 1999. Miocene evolution of atmospheric carbon dioxide. Paleoceanography 14, 273–292.

Popp, B.N., Laws, E.A., Bidigare, R.R., Dore, J.E., Hanson, K.L., Wakeham, S.G., 1998. Effect of phytoplankton cell geometry on carbon isotopic fractionation. Geochim. Cosmochim. Acta 62, 69–77.

Popp, B.N., Takigiku, R., Hayes, J.M., Louda, J.W., Baker, E.W., 1989. The post-Paleozoic chronology and mechanism of ^{13}C depletion in primary marine organic matter. Am. J. Sci. 289, 436–454.

Pratt, L.M., 1985. Isotopic studies of organic matter and carbonate in rocks of the Greenhorn marine cycle. In: Pratt, L.M., Kauffman, E.G., Zelt, F.B. (Eds.), Fine-Grained Deposits and Biofacies of the Cretaceous Western Interior Seaway: Evidence of Cyclic Sedimentary Process, Society of Economic Paleontologists and Mineralogists Field Trip Guidebook. SEPM, Tulsa, pp. 38–48.

Pratt, L.M., Arthur, M.A., Dean, W.E., Scholle, P.A., 1993. Paleo-oceanographic cycles and events during the Late Cretaceous in the Western Interior Seaway of North America. In: Caldwell, W.G.E., Kauffman, E.G. (Eds.), Cretaceous Evolution of the Western Interior Basin of North America. Geol. Assoc. Canada Spec. Pap. 39, pp. 333–353.

Salnikov, B.A., Tikhomolov, Y.I., 1987. A description of the section. In: Poyarkova, Z.N. (Ed.), Reference Section of Cretaceous Deposits in Sakhalin (Naiba Section). Trans. Acad. Sci. USSR, Leningrad 16, pp. 13–49 (in Russian).

Scholle, P.A., Arthur, M.A., 1980. Carbon Isotope fluctuations in Cretaceous pelagic limestones: Potential stratigraphic and petroleum exploration tool. Am. Assoc. Pet. Geol. Bull. 64, 67–87.

Shibata, K., Maeda, H., Uchiumi, S., 1997. Age of the Cenomanian–Turonian boundary in Hokkaido. J. Geol. Soc. Japan 103, 669–675.

Shigeta, Y., Maeda, H., Uemura, K., Solov'yov, A.V., 1999. Stratigraphy of the Upper Cretaceous System in the Kril'on Peninsula, south Sakhalin, Russia. Bull. Natl. Sci. Museum Ser. C 25, 1–27.

Stoll, H.M., Schrag, D.P., 2000. High-resolution stable isotope records from the Upper Cretaceous rocks of Italy and Spain: Glacial episodes in a greenhouse planet? GSA Bull. 112, 308–319.

Tanabe, K., Hirano, H., Matsumoto, T., Miyata, Y., 1977. Stratigraphy of the Upper Cretaceous deposits in the Obira area, northeastern Hokkaido (In Japanese with English abstract). Sci. Rep. Dept. Geol. Kyushu Univ. 12, 181–202.

Toshimitsu, S., Matsumoto, T., Noda, M., Nishida, T., Maiya, S., 1995. Towards an integrated mega-, micro- and magnetostratigraphy of the Upper Cretaceous in Japan (in Japanese with English abstract). J. Geol. Soc. Japan 101, 19–29.

Vereshchagin, V.N., 1961. Scheme on stratigraphy of Cretaceous deposits of Sakhalin. In: Vossoyevich, N.B. (Ed.), Decisions of Interdepartmental Meeting on Development of Unified Stratigraphical Schemes for Sakhalin, Kamchatka, Kuril and Commandor Islands. Gostoptekhizdat, Leningrad, p. 11 (in Russian).

Voigt, S., Wiese, F., 2000. Evidence for Late Cretaceous (Late Turonian) climate cooling from oxygen-isotope variations and palaeobiogeographic change in Western and Central Europe. J. Geol. Soc. London 157, 737–743.

Wani, R., Hirano, H., 2000. Upper Cretaceous biostratigraphy in the Kotanbetsu area, northwestern Hokkaido (in Japanese with English abstract). J. Geol. Soc. Japan 106, 171–188.

Zakharov, Y.D., Grabovskaya, V.S., Kalishevich, T.G., 1984. Succession of the Late Cretaceous marine assemblages in south Sakhalin and its climatic characteristics in the northwestern Pacific. In: Systematics and Evolution of Invertebrates in the Far East. Inst. Biol. Pedology, Far East Sci. Center, Akademiya Nauka, Vladivostok, pp. 41–90 (in Russian).

Zonova, T.D., 1987. Inoceramus. In: Poyarkova, Z.N. (Ed.), Reference Section of Cretaceous Deposits in Sakhalin (Naiba Section). Trans. Acad. Sci. USSR, Leningrad 16, pp. 63–75 (in Russian).